



OPEN

Differential interactions of *Rickettsia* species with tick microbiota in *Rh. sanguineus* and *Rh. turanicus*

Apolline Maitre^{1,2,3,11}, Myriam Kratou^{4,11}, Ivan Corona-Guerrero^{5,6,11}, Lianet Abuin-Denis^{1,7}, Lourdes Mateos-Hernández¹, Juan Mosqueda^{5,6}, Consuelo Almazan^{5,6}, Mourad Ben Said^{4,8}, Elianne Piloto-Sardiñas^{1,9}, Dasiel Obregon¹⁰✉ & Alejandro Cabezas-Cruz¹✉

Tick-borne rickettsioses, caused by Gram-negative bacteria of the *Rickettsia* genus, pose a growing global threat, with various arthropod vectors contributing to their transmission. Understanding the complex interactions within tick microbiota, including the role of *Rickettsia* species, is crucial for elucidating the dynamics of rickettsial diseases. Here, we investigate the taxonomic profiles and co-occurrence networks of *Rickettsia* in *Rh. sanguineus* sensus lato (s.l.) and *Rh. turanicus* ticks, revealing significant differences in community composition and local connectivity of *Rickettsia* species. While the microbiota of both tick species share common taxa, distinct differences in relative abundance and network topology suggest unique ecological niches. Moreover, robustness analysis demonstrates varying resilience to perturbations, indicating different strategies for network organization. Our findings also highlight metabolic differences between tick species, suggesting potential implications for *Rickettsia* interactions. Overall, this study provides insights into the intricate microbial landscape within ticks, shedding light on the functional redundancy and metabolic pathways associated with *Rickettsia*, thus advancing our understanding of tick-borne diseases.

Rickettsioses are vector-borne diseases caused by obligate intracellular Gram-negative bacteria within the *Rickettsia* genus, presenting an emergent growing global threat¹. Indeed, rickettsial bacteria have developed adaptations to diverse environmental conditions, including various arthropod vectors (i.e. ticks, fleas, lice, and mites²), and display a spectrum of mutualistic and pathogenic interactions³. These bacteria employ transmission patterns that can involve either strict vertical transmission or a combination of horizontal and vertical transmission routes². Pathogenic *Rickettsia* species have adapted to their specific vectors, evaded immune responses, persisted in essential organs, and exploited arthropod molecules⁴. Variations in transmission mechanisms within the genus explain why some *Rickettsia* species are virulent with horizontal transmission, while others are harmless endosymbionts with vertical transmission².

For decades, rickettsial pathogens have emerged and re-emerged alongside vector-borne rickettsial diseases, posing a threat to human and animal health worldwide. The significance of tick-associated rickettsial pathogens has grown substantially in the past 25 years, highlighting the evolution of these infections¹. In Palestine, a study

¹ANSES, INRAE, Ecole Nationale Vétérinaire d'Alfort, UMR BIPAR, Laboratoire de Santé Animale, 94700 Maisons-Alfort, France. ²INRAE, UR 0045 Laboratoire de Recherches sur le Développement de l'Élevage (SELMET-LRDE), 20250 Corte, France. ³EA 7310, Laboratoire de Virologie, Université de Corse, Corte, France. ⁴Laboratory of Microbiology, National School of Veterinary Medicine of Sidi Thabet, University of Manouba, 2010 Manouba, Tunisia. ⁵Immunology and Vaccines Laboratory, C. A. Facultad de Ciencias Naturales, Universidad Autónoma de Querétaro, Querétaro, Mexico. ⁶C.A. Salud Animal y Microbiología Ambiental. Facultad de Ciencias Naturales, Universidad Autónoma de Querétaro, Querétaro, Mexico. ⁷Animal Biotechnology Department, Center for Genetic Engineering and Biotechnology, Avenue 31 between 158 and 190, P.O. Box 6162, 10600 Havana, Cuba. ⁸Department of Basic Sciences, Higher Institute of Biotechnology of Sidi Thabet, University of Manouba, 2010 Manouba, Tunisia. ⁹Direction of Animal Health, National Center for Animal and Plant Health, Carretera de Tapaste y Autopista Nacional, Apartado Postal 10, 32700 San José de Las Lajas, Mayabeque, Cuba. ¹⁰School of Environmental Sciences, University of Guelph, Guelph, ON, Canada. ¹¹These authors contributed equally: Apolline Maitre, Myriam Kratou and Ivan Corona-Guerrero. ✉email: dasielogv@gmail.com; alejandro.cabezas@vet-alfort.fr

found that the rickettsial spotted-fever-group was detected in approximately 17% of the hard ticks collected from domestic animals⁵. The ticks *Rhipicephalus sanguineus* sensu lato (s.l.) and *Rhipicephalus turanicus* are commonly found on the same hosts (such as dogs, sheep and goats^{5,6}) and are morphologically close⁷. Many tick borne-bacteria (e.g. *Anaplasma platys*, *Anaplasma* spp., *Ehrlichia canis*, *Bartonella rochalimae*, *Bartonella chomelii*, *Bartonella koehlerae*^{8,9}), viruses (canine parvovirus¹⁰) and protozoa (e.g. *Theileria ovis*, *Babesia ovis*, *Babesia vogeli*, *Heptazoon canis*^{6,11}) have been identified in these two tick species. Notably, these findings underscored the significant role of *Rh. sanguineus* s.l. as the most prevalent species, infesting a diverse range of mammals, including dogs, sheep, goats, and horses. However, Erekat et al.⁵ have noted that the primary vector responsible for the transmission of SFG rickettsiae in this study was *Rh. turanicus*.

Numerous species of *Rickettsia* (i.e. *R. conorii*, *R. felis*, *R. africae*, *R. massiliae* and *R. sibirica mongolitimonae*^{5,12}) were found in *Rhipicephalus* ticks in the region. A phenomenon of rickettsial exclusion was observed by Burgdorfer et al.¹³, where the infection of *R. peacockii* in *Dermacentor andersoni* ticks blocked the ovarian infection of the pathogen *R. rickettsii*. Similar blocking phenomena of a rickettsial pathogen by another rickettsial species have been reported in different other tick species^{14,15}. However, the occurrence rickettsial exclusion appears to be complex, as reports of this absence have also been documented¹⁶. Further investigation is warranted to elucidate the interactions among pathogenic and non-pathogenic rickettsial species, as well as their interactions with other bacterial species within the tick microbiota.

Besides, tick microbial community is an important actor in the colonization and transmission of tick-borne diseases¹⁷. When a pathogen enters the tick's organs through blood meals, it faces a hostile environment due to midgut immunity^{2,18}. The newly acquired pathogen interacts with the tick's microbial midgut and will be able to persist in the ectoparasite's body. For successful transmission to a healthy host, the pathogen must migrate to the salivary glands and interface with distinct microbiota. The microbiota of *Rh. sanguineus* s.l. and *Rh. turanicus* is mainly composed of *Coxiella* and *Rickettsia* species^{7,19,20}. Rickettsial endosymbionts have a major role in the tick's microbiota, potentially providing nutritional symbiosis². Nonetheless, the presence of *Rickettsia helvetica*, an emerging pathogen of the spotted fever group, was reported to affect *Ixodes ricinus* microbiota by reducing its diversity and microbial interactions²¹. However, in both *Hyalomma marginatum* and *Rhipicephalus bursa* ticks originating from the same region, the presence of rickettsial pathogens appears to promote the prominence of certain bacterial taxa within the tick microbiota. This prominence plays a crucial role in maintaining community stability and may potentially facilitate the colonization of *Rickettsia*²².

Despite their lower abundance, certain microbial members significantly influence their environments²³. Network analysis offers profound insights into these effects, particularly elucidating the complex relationships between *Rickettsia* pathogens and the bacterial microbiota in questing ticks and those feeding on domestic animals. It also helps identify key factors driving *Rickettsia*'s interactions within these communities²⁴. This analytical approach aims to reveal the dynamics and nature of bacterial interactions, enhancing our understanding of community assembly, stability, and the behavioral intricacies of such complex systems²⁴. Specifically, by analyzing microbial networks, in this study we seek to understand the interactions of *Rickettsia* at both the taxonomic and functional levels, elucidating their potential implications for microbial fitness, composition, and metabolic functionalities.

Although the composition of microbiota is associated with the metabolic pathways expressed within ticks, research²⁵ has shown that despite the lack of shared taxa in the microbiota, the majority of metabolic pathways are still expressed. Therefore, the microbiota can exhibit high diversity while contributing to the same metabolic pathways²⁵. Furthermore, it has been demonstrated that a limited set of taxa can fulfill the majority of metabolic requirements for ticks, even in the face of environmental stress²⁶. This study aims to investigate whether *Rickettsia* associated with different taxa exhibit similar functions, thereby exploring the functional redundancy of the microbiome in the presence of *Rickettsia*. Ultimately, we aim to elucidate the metabolic pathways through which *Rickettsia* interacts with the broader microbiome, thus advancing our understanding of the microbial landscape within ticks and their hosts.

Results

Taxonomic profiles of *Rh. sanguineus* s.l. and *Rh. turanicus* microbiota

The analysis of beta and alpha diversity revealed that the microbiota of *Rh. sanguineus* s.l. and *Rh. turanicus* did exhibit significant differences in community composition, by analyzing the Bray–Curtis dissimilarity index, (Permanova, $p = 0.04$, $F = 1.79$; Fig. 1a), but the species richness (Kruskal–Wallis, $p > 0.05$; Fig. 1b) did not have significant differences. The most prevalent bacterium found in the microbiota across both studied tick species was *Coxiella burnetii*, with a prevalence rate of 90% (Fig. 1c). Interestingly, six *Rickettsia* species are present as the most prevalent taxa of the microbiota (from highest to lowest prevalent: *R. rickettsii*, *R. conorii*, *R. sibirica*, *R. massiliae*, *R. felis* and *R. bellii*; Fig. 1c). Within the dataset of 1263 identified taxa across all samples, 280 were unique to *Rh. sanguineus* s.l. microbiota, 49 were unique to *Rh. turanicus* microbiota, and 934 were shared between both tick species (Fig. 1d). From those common taxa, 15 presented significantly different relative abundances between the two tick species, including 9 *Corynebacterium* and 3 *Staphylococcus* species (Welch's *t*-test with Benjamini–Hochberg correction, $p < 0.05$; Fig. 1e). The 15 taxa were significantly more abundant in *Rh. turanicus* than in *Rh. sanguineus* s.l. (Fig. 1e). Notably, two *Rickettsia* species (*R. akari* and *R. massiliae*) exhibited significantly distinct relative abundance between the two tick microbiota (Welch's *t*-test, $p < 0.05$; Fig. 1f). Other *Rickettsia* species did not exhibit significantly different relative abundance (Welch's *t*-test, $p > 0.05$; Fig. 1f), but all *Rickettsia* species (i.e. *R. africae*, *R. akari*, *R. bellii*, *R. canadensis*, *R. conorii*, *R. felis*, *R. massiliae*, *R. monacensis*, *R. peacockii*, *R. prowazekii*, *R. rickettsia*, *R. sibirica* and *R. typhi*) were more abundant in the microbiota of *Rh. turanicus* compared to *Rh. sanguineus* s.l. microbiota (Fig. 1f).

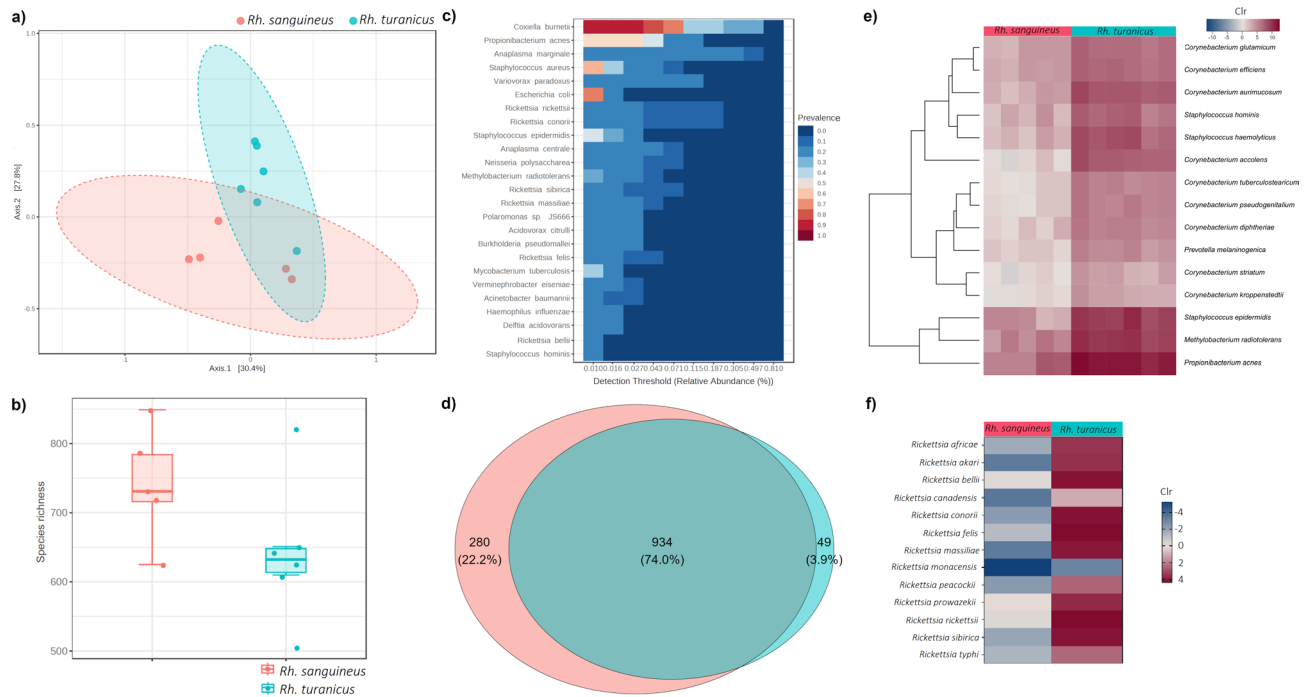


Fig. 1. Comparative analysis of microbial diversity at the species level in *Rh. sanguineus* s.l. and *Rh. turanicus*. **(a)** PCoA ordination plot showing microbial community structure variation between the two tick species along the primary axes (Permanova, $p=0.04$, $F=1.79$). Each point denotes a sample, distinguished by tick species, with 95% confidence intervals represented by ellipses. **(b)** Species richness (total microbial taxa) for each tick species, indicating the median, interquartile range, and outliers. No statistically significant differences were noted (Kruskal–Wallis, $p>0.05$). **(c)** Core microbiome heatmap reveals the prevalence of shared taxa across all tick samples at different detection thresholds, presented as relative abundance percentages. Taxa are organized in descending order based on average prevalence. **(d)** Venn diagram of shared and unique microbial taxa in both tick species, with the percentage of each relative to the combined taxa detected. **(e)** Comparison of differential taxa abundance between the two ticks species. The color gradient represents the clr values, with each row corresponding to a microbial species, and each column to a tick sample. Only species exhibiting a statistically significant difference between the two tick species are compared (Welch's t-test with Benjamini–Hochberg correction, $p<0.05$). **(f)** Comparison of differential *Rickettsia* abundance between the two ticks species. The color gradient represents the clr values, with each row corresponding to a *Rickettsia* species, and each column to a tick group, (pink for *Rh. sanguineus* s.l. and blue for *Rh. turanicus*).

Local connectivity of *Rickettsia* species in *Rh. sanguineus* s.l. and *Rh. turanicus* microbial communities

Microbial co-occurrence networks of *Rh. sanguineus* s.l. (Fig. 2a) and *Rh. turanicus* (Fig. 2b) demonstrated topological differences. *Rhipicephalus sanguineus* s.l. network boasted a higher number of nodes and edges compared to *Rh. turanicus* (1388 vs 921 nodes and 53,520 vs 7804 edges respectively; Fig. 2a,b; Table 1). Moreover, *Rh. sanguineus* s.l. displayed a greater proportion of negative interactions compared to *Rh. turanicus* (7.3% vs 0.4% respectively; Fig. 2a,b; Table 1). Additionally, *Rh. sanguineus* s.l. microbial network showed stronger connectivity (average degree = 77.12, average path length = 3.40; Table 1), in contrast to *Rh. turanicus* nodes (average degree = 16.95, average path length = 4.85; Table 1). In the two microbial networks, the local connectivity of *Rickettsia* species is different. In *Rh. sanguineus* s.l. microbiota, 9 species of *Rickettsia* are present and do not cluster together (Fig. 2a). In comparison, in *Rh. turanicus* microbiota, 12 species of *Rickettsia* are present and cluster together, except for *R. massiliae* (Fig. 2b).

A 'Core Associated Network' ('CAN') was constructed featuring the co-occurrence relations that are present in *Rh. sanguineus* s.l. and *Rh. turanicus* microbial network (Fig. 2c). The CAN comprises 1631 edges that connect 430 nodes, which represent 2.7% of the total number of edges (Fig. 2d) and 22.9% of the total number of nodes (Fig. 2e). This low number of similar edges demonstrates that the two ticks' microbiota have a distinct structure. For the *Rickettsia* species, three *Rickettsia* (*R. africanae*, *R. sibirica* and *R. peacockii*) have common relations (two positive co-occurrence correlations) between the microbiota of the two ticks species (Fig. 2c).

To compare the hierarchical organization of the two tick species, the Jaccard index was used to measure similarity of the most central nodes between *Rh. sanguineus* s.l. and *Rh. turanicus*. For all the centrality metrics measured, the Jaccard index was below 0.4 (Table 2) which demonstrates the dissimilarity of sets of most central nodes. Moreover, a significant group difference was observed for the degree, closeness centrality, eigenvector centrality and hub taxa ($P(\leq \text{Jacc}) < 0.001$; Table 2). Similarly, the 'Adjusted rand index' (ARI) (0, p -value = 0.96) indicates dissimilarity of clustering which is consistent with what is observed in Fig. 2a and b. After in silico removal of *Rickettsia* species in the microbial networks, no significant changes were observed in the Jaccard

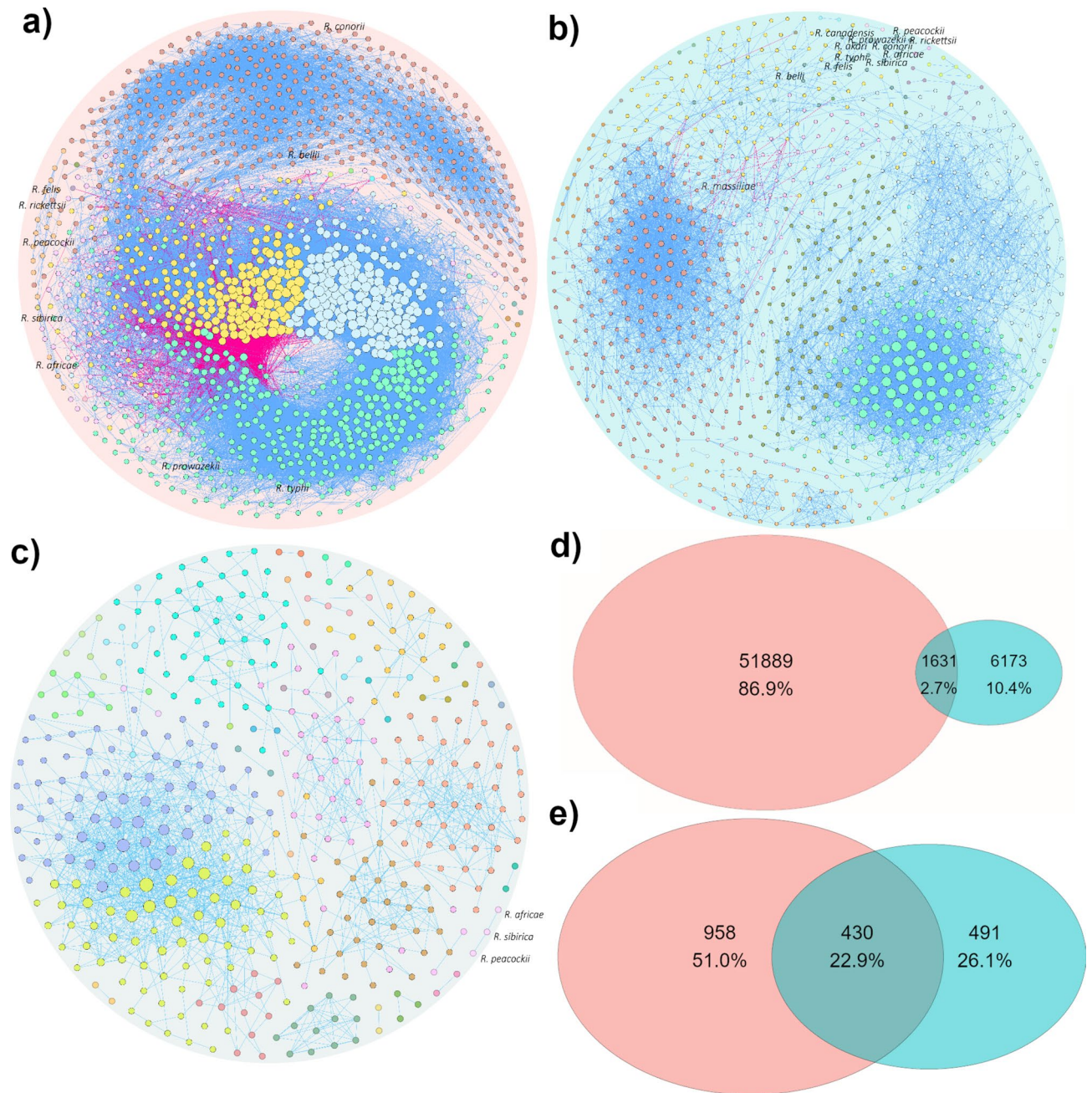


Fig. 2. Co-occurrence microbial network of *Rh. sanguineus* s.l. and *Rh. turanicus*. Global co-occurrence network of (a) *Rh. sanguineus* s.l. and (b) *Rh. turanicus* microbiota. (c) Core network (shared co-occurrence interactions) of *Rh. sanguineus* s.l. and *Rh. turanicus* microbiota. Nodes correspond to species and connecting edges correspond to a positive (blue) or negative (red) interaction between two nodes. Only nodes with at least one co-occurrence interaction are represented. Nodes colors correspond to modularity class metric. Nodes with the same color belong to the same module of co-occurring species. Size of the nodes corresponds to the eigenvector centrality of each species. The topological features of the corresponding networks are presented in Table 1 and the comparison of their most central nodes in Table 2. Venn diagram comparison of the number of shared (d) edges and (e) nodes between *Rh. sanguineus* s.l. (pink ellipse) and *Rh. turanicus* (blue ellipse) microbial networks. Numerals represent the number and percentage of nodes or edges that are *Rh. sanguineus*-exclusive, shared and *Rh. turanicus*-exclusive respectively.

index (Table 3) and the ARI (-0.007 , p -value = 0.202) although the absence of *Rickettsia* taxa tended to further distance the hierarchical organization of the two tick's microbiota. To compare the most central taxa of the two tick's microbiota, keystone taxa were calculated. A total of 54 keystone taxa within *Rh. sanguineus* s.l. microbiota and eight within *Rh. turanicus* microbiota were identified, as summarized in Supp. Table 1. It is noteworthy that there were no keystone taxa shared between the microbiota of both tick species which is consistent with the previous results.

Topological features	<i>Rh. sanguineus</i> s.l.	<i>Rh. turanicus</i>
Nodes	1388	921
Edges	53,520	7804
Positive	49,629 (92.7%)	7776 (99.6%)
Negative	3891 (7.3%)	28 (0.4%)
Modularity	0.61	0.64
Number of communities	19	27
Network diameter	14	17
Average path length	3.40	4.85
Average degree	77.12	16.95
Weighted degree	56.26	13.75
Clustering coefficient	0.57	0.52
LCC size	1384 (99.7%)	852 (92.5%)

Table 1. Topological features of the *Rh. sanguineus* s.l. and *Rh. turanicus* microbiota networks.

	Jaccard index	P (\leq Jacc)	P (\geq Jacc)
Degree centrality	0.25	0***	1
Betweenness centrality	0.37	0.954	0.054
Closeness centrality	0.24	0***	1
Eigenvector centrality	0.19	0***	1
Hub taxa	0.19	0***	1

Table 2. Jaccard index results for *Rh. sanguineus* s.l. and *Rh. turanicus* microbiota networks. *** $p < 0.05$.

	Jaccard index	P (\leq Jacc)	P (\geq Jacc)
Degree centrality	0.26	0***	1
Betweenness centrality	0.37	0.958	0.051
Closeness centrality	0.25	0***	1
Eigenvector centrality	0.24	0***	1
Hub taxa	0.24	0***	1

Table 3. Jaccard index results for *Rh. sanguineus* s.l. and *Rh. turanicus* microbiota networks without *Rickettsia*. *** $p < 0.05$.

Co-occurrence networks robustness

The robustness analysis was conducted to assess the resilience of co-occurrence networks for both *Rh. sanguineus* s.l. and *Rh. turanicus* in response to both, the removal or the addition of nodes. The systematic removal of nodes demonstrated that *Rh. turanicus* microbiota assembly was less robust than *Rh. sanguineus* s.l. (Fig. 3a–d). To reach 50% of connectivity loss, the fraction of nodes removed is smaller in *Rh. turanicus* compared with *Rh. sanguineus* s.l. for all removal strategies tested, namely random (0.25 vs 0.30 respectively, Fig. 3a), betweenness (0.15 vs 0.27 respectively, Fig. 3b), degree (0.25 vs 0.3 respectively, Fig. 3c) and cascading failure (0.01 vs 0.10 respectively, Fig. 3d). The analysis of changes in the Average Path Length (APL) and Largest Connected Component (LCC) size in response to node addition confirmed that *Rh. sanguineus* s.l. is more robust than *Rh. turanicus*. In *Rh. turanicus* network, the APL stays higher than *Rh. sanguineus* s.l. network even after the addition of 1000 nodes (Fig. 3e), indicating a less connected and compact network. A low LCC value is also an indicator of less robust and stable microbiota, like it is the case for *Rh. turanicus* network compared to *Rh. sanguineus* s.l. (Fig. 3f).

Local connectivity of *Rickettsia* spp. in the tick microbiota

The place of *Rickettsia* taxa in the two tick's microbiota was compared regarding the degree and betweenness value of all of the members of the microbiota. For the two tick's microbiota, the majority of taxa present low degree and low betweenness centrality (45.8% for *Rh. sanguineus* s.l. and 56.8% for *Rh. turanicus*; Fig. 4a,b). Four of the ten *Rickettsia* present in *Rh. sanguineus* s.l. exhibit high betweenness centrality and low degree (i.e. *R. africae*, *R. peacockii*, *R. prowazekii* and *R. typhi*; Fig. 4a), the other six present low degree and low betweenness centrality. In *Rh. turanicus* microbiota, *R. massiliae* presents high degree and high betweenness centrality value (Fig. 4b), and two *Rickettsia* present high betweenness centrality and low degree (*R. akari* and *R. bellii*; Fig. 4b).

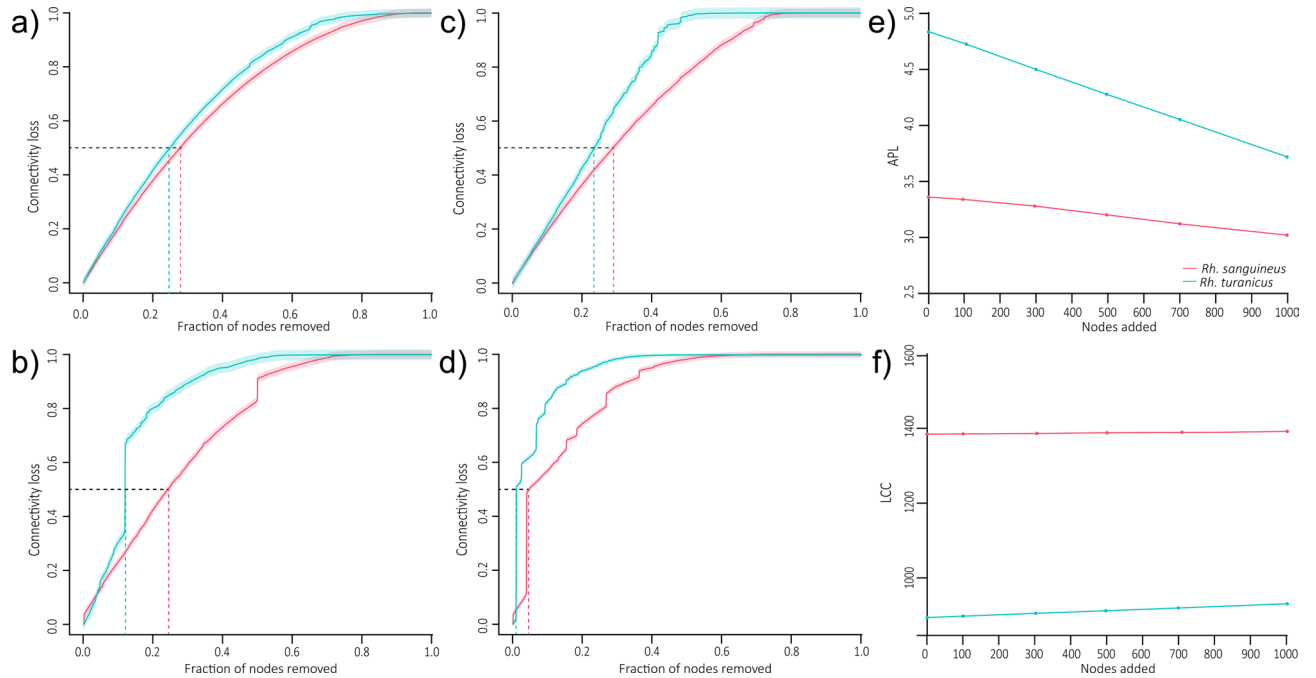


Fig. 3. Comparison of the robustness of *Rh. sanguineus* s.l. and *Rh. turanicus* microbial networks. Robustness test to assess the vulnerability of networks to node removal for the *Rh. sanguineus* s.l. (pink) and *Rh. turanicus* (blue) networks using (a) random, (b) betweenness, (c) degree and (d) cascading methods. X-axis represents the fraction of nodes removed from the network and Y-axis represents the fraction of connectivity loss. The solid line represents the fraction of nodes removed to connectivity loss-ratio and the shaded area represents the standard error. The black dashed line represent the level of connectivity loss of 0.5, colored dashed line represent the corresponding level of fraction of node removed to reach 0.5 of connectivity loss. Robustness test to assess the resiliency of networks to node addition for the *Rh. sanguineus* s.l. (pink) and *Rh. turanicus* (blue) networks. X-axis represents the number of nodes added from 0 to 1000 and Y-axis represents (e) the average path length or (f) the Largest connected component size.

Those results demonstrate that *Rickettsia* pathogens do not have the same role in the microbiota of ticks, while *R. massiliae* seems to influence in the microbiota assembly of *Rh. turanicus*.

To analyze the co-occurrence relations of *Rickettsia* within the genera and with the rest of the microbiota, subnetworks centered on Rickettsial associations were produced. Within the co-occurrence network of *Rh. sanguineus* s.l., Rickettsial nodes exhibited limited connections to each other, except for *R. sibirica*, which was linked to both *R. peacockii* and *R. africae* (Fig. 4c). Moreover, Rickettsial species were linked with 94 external taxa (Fig. 4c). In contrast, Rickettsial nodes within the *Rh. turanicus* network were intricately interlinked with each other (32 edges between Rickettsial species; Fig. 4d). Only *R. bellii*, *R. felis*, and *R. massiliae* shared edges with non-Rickettsial taxa, totaling 18 neighbors in all (Fig. 4d).

Metabolic profile of *Rh. sanguineus* s.l. and *Rh. turanicus* microbiota

An analysis of the metagenomics data was conducted to obtain a metabolic analysis of the genes expressed by the members of the microbiota of each tick. A total of 5080 metabolic functions were found for the two tick species, from which 3093 were shared between the two tick species, 1719 were only present in *Rh. sanguineus* s.l. metabolism and 267 only present in *Rh. turanicus* (Fig. 5a). For the functions only present in *Rh. sanguineus* s.l., 235 are carbohydrates, 163 are Clustering based subsystems, 123 are Metabolism of aromatic compounds and 109 are Amino acids derivatives (Supp. Table 2). The 971 other functions were shared with 23 Level 3 SEED functions (Supp. Table 2). For the functions only present in *Rh. turanicus*, 41 are carbohydrates, 29 are Clustering based subsystems, 19 are Amino acids derivatives, 17 are Virulence, disease and defense and 16 are Regulation and cell signaling (Supp. Table 2). The 145 other functions are shared with 19 Level 3 SEED functions (Supp. Table 2). The beta diversity analysis showed no significant difference in clustering of the samples by tick species (Permanova, $p = 0.424$, stress = 0.05, $F = 0.89$; Fig. 5b). Differential abundance analysis of the gene expression highlighted 41 genes with significant difference (Wald test, $p < 0.05$; Fig. 5c). Among these, thirteen genes showed significant higher abundance in *Rh. sanguineus* s.l., including five Amino acids and derivatives and three Carbohydrate functions whereas 28 genes were significantly more abundant in *Rh. turanicus*, including four DNA metabolism, three Carbohydrates, three Clustering-based subsystems, three Fatty acids, lipids, and isoprenoids, three Protein metabolism and three RNA metabolism functions (Supp. Table 3).

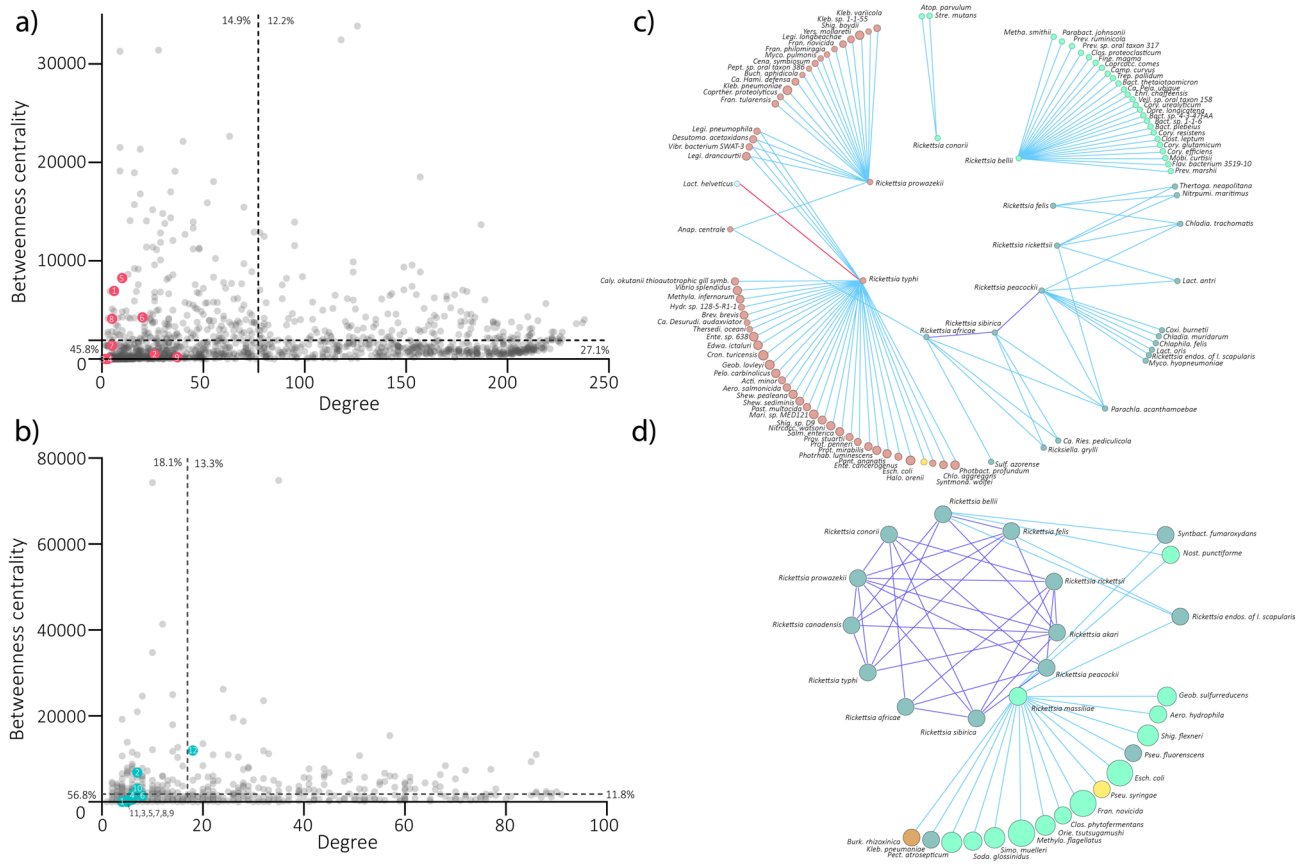


Fig. 4. Comparison of place and neighbors of Rickettsial species in the microbial networks of *Rh. sanguineus* s.l. and *Rh. turanicus*. Scatterplot of the degree and betweenness centrality of taxa in (a) *Rh. sanguineus* s.l. and (b) *Rh. turanicus* microbiota. Pink and blue dots represent *Rickettsia* spp. in *Rh. sanguineus* s.l. and *Rh. turanicus* respectively (1: *Rickettsia africana*. 2: *Rickettsia bellii*. 3: *Rickettsia conorii*. 4: *Rickettsia felis*. 5: *Rickettsia peacockii*. 6: *Rickettsia prowazekii*. 7: *Rickettsia rickettsii*. 8: *Rickettsia sibirica*. 9: *Rickettsia typhi*. 10: *Rickettsia akari*. 11: *Rickettsia canadensis*. 12: *Rickettsia massiliae*). The dash line represents the degree and betweenness centrality average. Direct neighbors of *Rickettsia* spp. present in the (c) *Rh. sanguineus* s.l. and (d) *Rh. turanicus* microbial network. Nodes correspond to species and connecting edges correspond to a positive (blue) or negative (red) co-occurrence interaction between two nodes. Positive edges shared between two Rickettsial species are highlighted in dark blue. In each network, nodes with the same colors belong to the same module and the node size is correlated with the eigenvector centrality value. Abbreviations are listed in Supp. File 1.

Discussion

The tick microbiota’s contributions to tick physiology and the pathogen life cycle are crucial for understanding vector capacity^{17,27–29}. Studies have reported the taxonomic composition of midgut microbiota in various tick species, including *Rhipicephalus*, *Ixodes*, *Amblyomma*, *Haemaphysalis*, *Hyalomma*, and *Dermacentor*³⁰. Despite this taxonomic variability, certain bacterial taxa, such as *Arsenophonus*, *Candidatus Midichloria*, *Rickettsia*, and *Wolbachia*, are frequently identified in *Ixodes* and *Rhipicephalus* tick species³¹. Rickettsiales have evolved to adapt to diverse environmental conditions, including various arthropod vectors and mammalian hosts, displaying varying degrees of mutualism and pathogenicity^{3,32}. The tick microbiome consists of both pathogenic and non-pathogenic microbes, which interact synergistically within the tick vector, such as *Candidatus Midichloria mitochondrii* (CMM) and *Rickettsia parkeri*, or competitively, such as CMM and *Francisella*-like endosymbionts (FLE)³². Understanding the functional consequences of pathogen colonization by Rickettsial species within the tick vector and their transmission to hosts is essential, also an understanding of endosymbionts and their interactions with pathogenic microbes is necessary to decipher the molecular mechanisms involved in the colonization of tick vectors by pathogenic microbes to develop new paradigms targeting tick proteins to control ticks and tick-transmitted pathogens³².

In this study, we especially focus on the relation of Rickettsial species within the genera, and their interaction with the rest of the microbiota. Leveraging published data¹⁰ from tick microbiota metagenomics sequencing, we investigate the relationship of Rickettsial species within the genera and their interaction with the rest of the microbiota in *Rh. sanguineus* s.l. and *Rh. turanicus*. The original study of Ravi et al.¹⁰ primarily concentrated on assembling and characterizing the genomes of tick-borne pathogens and endosymbionts within ticks from four different taxa: *Rh. sanguineus* s.l., its close relative *Rh. turanicus*, *Haemaphysalis*, and *Hyalomma*, collected from various hosts, and documented significant pathogens within these vectors. Through DNA sequencing, they

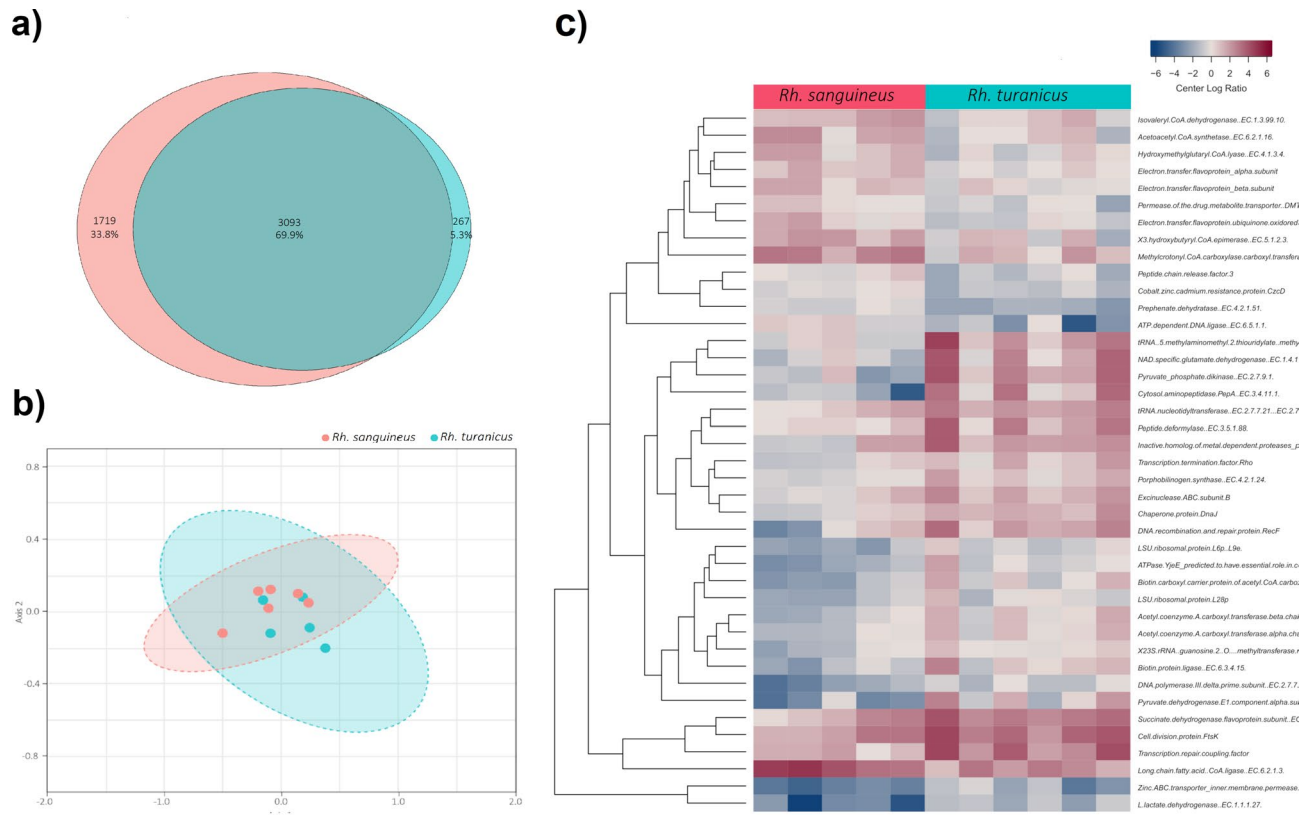


Fig. 5. Diversity and differential abundance of the metabolic pathways provided by *Rh. sanguineus* s.l. and *Rh. turanicus* microbiota. (a) Venn diagram representing unique and shared pathways of *Rh. sanguineus* s.l. (pink) and *Rh. turanicus* (blue) (b) Beta-diversity comparison between the pathways present in the *Rh. sanguineus* s.l. (pink) and *Rh. turanicus* (blue) microbiota samples using the Bray–Curtis dissimilarity index. Small circles represent samples and the ellipses represent the centroid for each group (Permanova, $p=0.424$, stress = 0.05, $F=0.89$). (c) Comparison of differential gene expression between *Rh. sanguineus* s.l. and *Rh. turanicus* microbiota samples. The color gradient indicates the clr value for the relative expression fold change of differentially expressed genes (presented in each row) for each microbiota sample (represented in each column). Only genes with a statistically significant expression difference between each tick species were presented (Wald test, $p < 0.05$).

unexpectedly identified canine parvovirus and an unsequenced pathogen, *Candidatus Rickettsia barbariae*¹⁰. Our investigation offers a comprehensive analysis of microbiota composition and network dynamics in *Rh. sanguineus* s.l. and *Rh. turanicus*, yielding key insights into the microbial ecology of these tick species. To achieve this, we used comparisons of diversity metrics, differential taxonomic abundance, and a network approach to explore the complexity of microbial communities including their organization, assembly, stability, and interactions. Additionally, we compared the robustness and topological features of the microbiota in both tick species and utilized diversity metrics to compare functional pathways involved in their microbial communities.

We found no significant differences in the alpha diversity, while the Bray–Curtis dissimilarity test was significantly different between the microbiota of *Rh. sanguineus* s.l. and *Rh. turanicus*. This finding suggests an equivalent microbial richness, but a significant dissimilarity in the relative abundance across the two conditions. This similarity of microbial richness might be due to phylogenetic closeness between *Rh. sanguineus* s.l. and *Rh. turanicus* tick species¹⁹. A similar result was in prior research that demonstrated a clustering of beta diversity in *Ixodes persulcatus* and *Ixodes ricinus*, distinct from *Dermacentor reticulatus*³³. However, the different bacterial composition observed between the two tick microbiota is consistent with previous findings^{22,34}, emphasizing the dependence of microbial composition on multiple factors, including tick species. Moreover, the different biological traits of the two tick species might explain this dissimilarity, with *Rh. turanicus* life cycle more dependent to environmental factor³⁵, impacting also the ticks microbiota. Their ecological niches differ, with *Rh. turanicus* commonly found in arid and semi-arid regions, whereas *Rh. sanguineus* s.l. is more prevalent in urban and peri-urban areas. These differing habitats expose the ticks to distinct microbial communities, which likely contribute to the observed differences in their microbiota.

It is noteworthy that all pathogenic Rickettsial taxa were more abundant in *Rh. turanicus* compared to *Rh. sanguineus* s.l., consistent with previous findings in the region³⁶. Although *Rh. sanguineus* s.l. harbors a greater number of microbial taxa, *Rh. turanicus* microbiota exhibited a higher relative abundance, particularly of *Corynebacterium* and *Staphylococcus* species. The presence of the canine parvovirus in one of the *Rh. sanguineus* s.l. tick sample might have an effect on the pathogenic *Rickettsia* presence by competing for resources or

ecological niche. The effect of the severe fever with thrombocytopenia virus on *Haemaphysalis* tick was analysed and demonstrated a reduction of operational taxonomic units and an alteration of the microbial composition³⁷. The dominance of *Coxiella burnetii* and the presence of diverse *Rickettsia* species across both tick species underscore the importance of these bacteria in the tick microbiome, potentially influencing tick survival, reproduction, and capacity for disease transmission^{7,38}. *Coxiella*-like endosymbionts (CLEs) are predominantly associated with female ticks, colonizing their Malpighian tubules and ovaries, with maternal transmission observed^{19,39}. While tissue tropism for *Rickettsia* sp. in *Rh. sanguineus* s.l. remains unclear, maternal transmission of these symbionts has been noted^{39–42}. Lalar et al. proposed a competitive colonization of the ovary between *Coxiella* sp. and *Rickettsia* sp.³⁹. Moreover, repeated horizontal transfers in *Rickettsia* may have conferred novel pathogenic traits, exemplified by *Coxiella burnetii*, which emerged from CLEs, causing Q fever⁴³.

The topological analysis of microbial co-occurrence networks revealed distinct patterns between the two tick species. *Rh. sanguineus* s.l. displayed a more intricate network structure with a higher number of nodes and edges, indicating a more interconnected and potentially robust microbiota. This complexity may confer advantages in adapting to environmental stressors or resisting pathogen invasion⁴⁴. In contrast, *Rh. turanicus* exhibited lower links and a higher abundance of Rickettsial pathogens compared to *Rh. sanguineus* s.l. The association between the presence of *Rickettsia* and low connectivity may describe a pattern of *Rickettsia* colonization or persistence in ticks. Indeed, a previous study²¹, demonstrated that the presence of the pathogenic *R. helvetica* in *I. ricinus* ticks was linked to a loss of microbial connectivity. Further analysis is needed to understand this phenomenon, especially if the presence of pathogenic *Rickettsia* alters the microbiota to facilitate infection, or if a less robust microbiota is more susceptible to acquire *Rickettsia*. However, we observed that the 'core bacterial microbiota' was not conserved between *Rh. sanguineus* s.l. and *Rh. turanicus*. Only three *Rickettsia* species, *R. africana*, *R. sibirica*, and *R. peacockii*, were common within the core microbiota. This suggests that the microbiota of these ticks have distinct structures, contradicting some studies that have shown conservation of core microbiota bacteria among closely related species, likely due to their essential roles in maintaining microbial community function⁴⁵.

The intricate microbial community residing in tick guts plays a crucial role in pathogen colonization and potentially influences tick fitness⁴⁶. Network robustness, reflecting the resistance of the tick microbiome to biological disturbance, is a property observed in various animal species, including arthropods^{46,47}. In this study, we perturbed the co-occurrence bacterial networks of *Rh. sanguineus* s.l. and *Rh. turanicus* by simulating the removal and addition of nodes in silico. We then compared the topology, connectivity, local centrality measures, robustness, and community assembly between the perturbed and original networks. Additionally, we may observe a phenomenon of colonization resistance within the ticks, where the microbiota's resistance against exogenous pathogenic microbes protects and stabilizes established communities⁴⁸, which was the case of *Rh. turanicus* that exhibited a less robust network, highlighting different network behaviors and resilience between *Rh. turanicus* and *Rh. sanguineus* s.l. The presence of Rickettsial endosymbionts often correlates with Rickettsial pathogens². Differences in the local connectivity of Rickettsial species within the networks underscore the nuanced roles these pathogens play within the tick microbiota, influencing community dynamics and potentially impacting disease transmission pathways. The position of *Rickettsia* within the microbiota varies depending on the tick species⁴⁹. For instance, a study²² on *Hyalomma marginatum* and *Rh. bursa* microbiota revealed that *Rickettsia* inhabited contrasting communities, potentially indicating different roles within the microbiota. However, despite this variability, the presence of *Rickettsia* was correlated with similar central taxa, potentially facilitating pathogen acquisition²². Moreover, *R. peacockii* is associated with the pathogen *R. rickettsii* or *R. buchneri* with *R. monacensis*³². Consistent with this, in our study, we observed co-occurrence connections among *Rickettsia* species and a higher abundance of these bacteria in *Rh. turanicus*. Conversely, when Rickettsial species lack co-occurrence interactions, the abundance of *Rickettsia* decreases, which was the case with *Rh. sanguineus* s.l.

Through reductive genome evolution, *Rickettsia* has undergone gene loss in metabolic pathways, resulting in a limited ability to synthesize amino acids and nucleotides, resembling symbiotic bacteria⁵⁰. To compensate for this loss, *Rickettsia* species have developed parasitic mechanisms, utilizing a diverse array of transport systems to acquire essential metabolites for survival and replication within the host cytosolic compartment⁵⁰. Thus, identifying specific metabolic pathways missing in *Rickettsia* may provide critical knowledge in gaps in developing an axenic medium that supports rickettsial extracellular replication and novel therapeutics that target essential transport mechanisms⁵⁰. Our metabolic analysis revealed distinct profiles between *Rh. sanguineus* s.l. and *Rh. turanicus*, with significant differences in genes associated with carbohydrates, amino acids, and virulence. These metabolic distinctions may reflect adaptations to different environmental conditions or host preferences⁵¹, potentially influencing tick feeding behavior, reproduction, and pathogen transmission. A previous study⁵² that assessed the reaction of *Rh. sanguineus* s.l. to stress (starvation), predicted a higher level of carbohydrate metabolism in stress condition. Consistent with this, our study observed an increase in carbohydrate metabolism pathways in the functional profile of *Rh. sanguineus* s.l. compared to *Rh. turanicus*. The regulation of the carbohydrate metabolism was also correlated with a resistance to oxidative stress⁵³. However, another study⁵⁴ demonstrated that the pathogen *Anaplasma phagocytophilum* was able to manipulate carbohydrate metabolism to facilitate infection in tick cells. This phenomenon was described for *I. scapularis* ticks⁵⁵.

The findings from our study have important implications for understanding the role of tick microbiota in disease transmission. The presence of primary pathogens such as *Coxiella burnetii* and various *Rickettsia* species, coupled with the intricate microbial networks observed, suggests that the tick microbiota may play a significant role in modulating tick-borne disease dynamics. Further research is needed to elucidate the functional roles of these microbial communities in pathogen transmission and tick physiology. While our study provides valuable functional metagenomic data, future research should focus on experimental settings that integrate metagenomics with other omics approaches, such as transcriptomics and proteomics. This integrated approach is essential to disentangle the roles of microbiome assembly and metabolic interdependence in the survival, replication, and transmission of pathogens. Understanding the molecular mechanisms underlying these interactions can provide

insights into how microbiota influence tick-borne disease dynamics and identify key microbial partners that support tick health and development, potentially revealing targets for disrupting tick populations and reducing disease transmission.

Conclusion

Our study elucidates the intricate relationships between *Rickettsia* species and the broader microbiome within *Rh. sanguineus* s.l. and *Rh. turanicus* ticks. By characterizing taxonomic profiles, co-occurrence networks, and metabolic pathways, we have gained valuable insights into the complexity of tick microbiota and its implications for rickettsial diseases. The distinct community compositions and network structures observed between tick species underscore the importance of considering ecological dynamics in understanding disease transmission. Furthermore, the differential metabolic profiles highlight potential mechanisms underlying *Rickettsia* interactions and their role in tick physiology. Moving forward, a deeper understanding of these interactions through experimental studies and omics approaches will be essential for developing targeted interventions to control rickettsial infections and mitigate the threat of tick-borne diseases.

Methods

Study design

The study aims to describe *Rh. sanguineus* s.l. and *Rh. turanicus* microbiota at a species level and to describe the role of *Rickettsia* species in the microbiota of the two tick species. A functional analysis of the metabolic genes directly provided to Rickettsial species will also be investigated. For this, *Rh. sanguineus* s.l. ($n = 5$) and *Rh. turanicus* ($n = 6$) samples were used from a previous study¹⁰. The ticks were collected in 2015 from dogs for *Rh. sanguineus* s.l. and from sheep for *Rh. turanicus* in Palestine farms, from Nablus ($n = 2$ *Rh. sanguineus* s.l. and $n = 3$ *Rh. turanicus*), from Tubas ($n = 3$ *Rh. sanguineus* s.l. and $n = 2$ *Rh. turanicus*) and from Hebron ($n = 1$ *Rh. turanicus*)¹⁰. Ticks were collected from their host and placed in 70% ethanol and then the DNA was extracted and sequenced by shotgun metagenomics sequencing¹⁰. Previous metagenomics analysis permitted to assess the presence of bacterial or viral pathogens. Coxiellaceae was found in *Rh. sanguineus* s.l. and *Rh. turanicus*, while Rickettsiaceae and Anaplasmataceae were predominantly found in *Rh. turanicus*¹⁰. Moreover, the canine parvovirus was found in one *Rh. sanguineus* s.l. tick¹⁰.

Processing of raw metagenomic sequences

Whole genome sequencing (WGS) sequences underwent preprocessing and annotation via the Metagenomic Rapid Annotations using subsystems technology (MG-RAST) web application server, utilizing pipeline version 4⁵⁶. Initially, raw sequences were subjected to quality control (QC) through SolexaQA software, employing the "Dynamic Trim" method for excising low-quality segments based on a minimum Phred score of 15 and allowing no more than 5 bases below this threshold⁵⁷. This step was followed by the elimination of artificial replicate sequences and singletons⁵⁸. Protein-coding regions were identified leveraging the M5nr database for a comprehensive, non-redundant amalgamation of multiple protein databases⁵⁹. The taxonomic origins of these regions were ascertained using the RefSeq database⁶⁰, while functional profiles were delineated based on the SEED subsystems. Annotation parameters adhered to the guidelines recommended by⁶¹, employing an MG-RAST: maximum e-value cut-off of $1e-5$, a minimum alignment length of 15 bp, and minimal identity cut-offs of 60% and 80% for taxonomic and functional profiling, respectively. This approach balanced sensitivity and accuracy. Abundance profiles were established using the 'Representative Hit Classification' method, with features identified as eukaryotic and viral sequences being excluded from the analysis.

Diversity indexes and taxa abundance

Beta diversity measures the variability of samples between different conditions to assess similarity of communities. To measure the microbial beta diversity, the Bray–Curtis dissimilarity index⁶² was used. Bray–Curtis tested the dissimilarity between two conditions, considering the relative abundance of taxa⁶². Bray–Curtis was measured using 'vegan' package⁶³ implemented on R studio⁶⁴. To statistically compare the two conditions, a PerMANOVA test ($p < 0.05$) was conducted using Past 4 (v. 4.08, 2001). Alpha-diversity analysis was based on microbial species richness for the two tick species. Alpha diversity was measured using MG-RAST⁵⁶, and statistically compared using Kruskal–Wallis test ($p < 0.05$).

To further compare the diversity of the two tick species microbiota, the core microbiome analysis, encompassing all samples, was conducted to identify taxa at varying prevalences ranging from 20 to 100%. This analysis was carried out using the web-based tool, MicrobiomeAnalyst⁶⁵. Moreover, a Venn diagram was built to visualize the shared taxa and the unique taxa present in each microbiota. The Venn diagram was built using 'VennDiagram' package⁶⁶ in R studio⁶⁴. Differential abundance analysis was used to compare significantly different taxa. Abundance values were measured as centered log ratio (clr) transformed values and t -test was realized using 'ANOVA-Like Differential Expression' ('ALDEx2') package⁶⁷ in R-studio⁶⁴. The heatmap with only statistically different taxa abundant (Benjamini–Hochberg corrected p -value⁶⁸) was constructed using 'heatmap.2'⁶⁹ package implemented in R studio⁶⁴. Differential abundance was also represented to compare the abundance of Rickettsial species between the two tick species. The clr values were calculated with 'ALDEx2', a t -test was performed and the average clr values of each *Rickettsia* (significant or not) in each condition were presented in a heatmap constructed with GraphPad Prism 9.0.2 (GraphPad Software).

Inference of co-occurrence networks analysis

To further explore the intricate system that microbiota is, a network approach was used to compare the two species microbiota. Networks are composed of nodes representing bacterial taxa at the species level and links

referring to positive or negative co-occurrence interactions between taxa. The networks were constructed using ‘Sparse Correlation for Compositional data’ (‘SparCC’) method⁷⁰ implemented in R studio⁶⁴. Links correlation coefficient magnitude threshold was >0.75 for positive and <-0.75 for negative co-occurrence interactions, as it is commonly used for microbial networks⁷¹ to obtain statistically meaningful results. Networks were visualized and topological features (i.e. number of nodes and edges, modularity, network diameter, average degree, weighted degree, clustering coefficient, and centrality metrics) were calculated using Gephi 0.10⁷². *Rh. sanguineus* s.l. and *Rh. turanicus* microbial network similarity in structure was compared using CAN. CAN network represents the intersection of similar links associated with the same taxa in the two microbial networks. Positive links represent edges that were positive in the two species networks. On the opposite, negative links represent edges that were negative in the two species network. CAN was constructed using ‘anuran’ toolbox⁷³ with the default parameters, implemented on python environment (Anaconda Software Distribution 2023). Shared proportion of links and nodes were represented in a Venn diagram using ‘VennDiagram’ package⁶⁶ implemented on R studio⁶⁴.

To test the similarity of the most central nodes between *Rh. sanguineus* s.l. and *Rh. turanicus*, the Jaccard index was used ($p < 0.05$). This index compared the similarity of nodes with a central place in the microbiota (i.e., high eigenvector, betweenness, degree, closeness centrality and hub taxa) of the two ticks’ microbial networks. Jaccard value goes from 0 (central nodes completely different) to 1 (sets of most central nodes equal). Jaccard statistically compares if the high central nodes are “less similar or equal” (p -value $P(J \leq j)$), or “higher similar or equal” (p -value $P(J \geq j)$) than the Jaccard value expected for two random microbial networks⁷⁴. Similarly to the Jaccard index, the ARI was calculated to statistically compare if the two microbial networks cluster similarly. ARI value goes from 0 (expected for two random clustering) to 1 (perfect agreement between clustering). A statistical two-tailed test was conducted with the null hypothesis that $ARI = 0$. The Jaccard index and the ARI were performed using ‘Network Construction and comparison for Microbiome data’ (‘Netcomi’)⁷⁵ package implemented on R studio⁶⁴.

Evaluation of the network robustness

The robustness analysis explores and compares the resistance of microbial networks to perturbations such as removal or addition of a substantial number of nodes. To compare the microbiota of the two tick species resistance to node removal, the connectivity loss depending on the fraction of nodes removed was calculated for four different node removal methods (i.e. random, degree, betweenness and cascading (recalculated betweenness) removal). The robustness was measured with ‘Network Strengths and Weaknesses Analysis’ (‘NetSwan’) package⁷⁶ implemented on R studio⁶⁴. Because the microbiota can be affected by various factors, such as environmental changes, it is crucial to test how the addition of new microbial species can affect the microbial network stability. Node addition was measured using Network Analysis⁷⁷, with igraph visualization package^{78,79} implemented on R studio⁶⁴. We quantified network connectivity after additions of 10,000 nodes using two metrics: the largest connected component (LCC) and the average path length (APL). To analyze the significance of differences in LCC and APL after node addition, we conducted one-sample Wilcoxon signed-rank test with p -values adjusted using the Benjamini–Hochberg correction⁶⁸ to minimize the false discovery rate. We also implemented bootstrapping techniques to generate confidence intervals for these metrics. A significance level was set at $p < 0.05$ to determine statistical relevance. GraphPad Prism 9.0.2 (GraphPad Software) was used for visualization of both metrics.

Connectivity of Rickettsial species in the microbiota

To compare the role of Rickettsial species between the two ticks microbiota, the degree and the betweenness centrality value were calculated for all of the taxa in each ticks microbiota, and the place of *Rickettsia* in the community assembly was observed. The degree and betweenness centrality values were collected with Gephi 0.10⁷² software and visualized with GraphPad Prism 9.0.2 (GraphPad Software). They were separated in four groups: i. low degree and low betweenness centrality, ii. low degree and high betweenness centrality, iii. high degree and low betweenness centrality, and iv. high degree and high betweenness centrality. The threshold was the average value (77.12 for degree and 1896.31 for betweenness centrality for *Rh. sanguineus* and 16.95 for degree and 1857.37 for betweenness centrality for *Rh. turanicus*). Furthermore, the place of Rickettsial species and their relation with members of the microbiota was investigated. Reference taxa networks were constructed, and only direct co-occurrence relations of Rickettsial species were represented. Direct co-occurrence correlations and visualization were done using Gephi 0.10⁷² software.

Comparison of gene diversity and abundance

To compare the metagenomics values of the two tick species, a Venn diagram was prepared to know which functions are unique to *Rh. turanicus* or to *Rh. sanguineus* s.l. and the one that are shared between the two tick species. The Venn diagram was conducted using the same method as for the taxa comparison. A beta diversity dissimilarity plot was constructed to see if the metagenomics gene population was similar between the two tick species or if they clustered separately. This analysis was conducted using the same method as for the taxa comparison. The significant (Wald test, $p < 0.05$) different genes were measured using DeSeq2 package⁸⁰ implemented on R studio⁶⁴, and visualized using heatmap.2⁶⁹ function implemented in R studio⁶⁴.

Data availability

The data that support this study results are available on the SRA repository (Bioproject No. PRJNA495172).

Received: 1 March 2024; Accepted: 28 August 2024

Published online: 05 September 2024

References

- Parola, P. *et al.* Update on tick-borne rickettsioses around the world: A geographic approach. *Clin. Microbiol. Rev.* **26**, 657–702 (2013).
- Laukaitis, H. J. & Macaluso, K. R. Unpacking the intricacies of *Rickettsia*-vector interactions. *Trends Parasitol.* **37**, 734–746 (2021).
- Kim, H. K. *Rickettsia*-host-tick interactions: Knowledge advances and gaps. *Infect. Immun.* **90**, e0062121 (2022).
- Helminiak, L., Mishra, S. & Kim, H. K. Pathogenicity and virulence of *Rickettsia*. *Virulence* **13**, 1752–1771 (2022).
- Eraqat, S. *et al.* Molecular detection and identification of spotted fever group Rickettsiae in ticks collected from the West bank, Palestinian territories. *PLoS Negl. Trop. Dis.* **10**, e0004348 (2016).
- Azmi, K. *et al.* Molecular detection of *Theileria*, *Babesia*, and *Hepatozoon* spp. in ixodid ticks from Palestine. *Ticks Tick Borne Dis.* **7**, 734–741 (2016).
- René-Martellet, M. *et al.* Bacterial microbiota associated with *Rhipicephalus sanguineus* (s.l.) ticks from France, Senegal and Arizona. *Parasit. Vectors* **10**, 416 (2017).
- Zaid, T. *et al.* Molecular characterization of *Anaplasma* and *Ehrlichia* in ixodid ticks and reservoir hosts from Palestine: A pilot survey. *Vet. Med. Sci.* **5**, 230–242 (2019).
- Eraqat, S. *et al.* Molecular evidence of *Bartonella* species in Ixodid ticks and domestic animals in Palestine. *Front. Microbiol.* **7**, 1217 (2016).
- Ravi, A. *et al.* Metagenomic profiling of ticks: Identification of novel rickettsial genomes and detection of tick-borne canine parvovirus. *PLoS Negl. Trop. Dis.* **13**, e0006805 (2019).
- Azmi, K. *et al.* Detection and molecular identification of *Hepatozoon canis* and *Babesia vogeli* from domestic dogs in Palestine. *Parasitology* **144**, 613–621 (2017).
- Mumcuoglu, K. Y., Keysary, A. & Gilead, L. Mediterranean spotted fever in Israel: A tick-borne disease. *Isr. Med. Assoc. J.* **4**, 44–49 (2002).
- Burgdorfer, W., Hayes, S. F. & Mavros, A. J. *Nonpathogenic rickettsiae in Dermacentor andersoni: a limiting factor for the distribution of Rickettsia rickettsii* Vol. Rickettsiae and rickettsial diseases (Academic Press, 1980).
- Macaluso, K. R., Sonenshine, D. E., Ceraul, S. M. & Azad, A. F. Rickettsial infection in *Dermacentor variabilis* (Acari: Ixodidae) inhibits transovarial transmission of a second *Rickettsia*. *J. Med. Entomol.* **39**, 809–813 (2002).
- Sakai, R. K. *et al.* Experimental infection with *Rickettsia rickettsii* in an *Amblyomma dubitatum* tick colony, naturally infected by *Rickettsia bellii*. *Ticks Tick Borne Dis.* **5**, 917–923 (2014).
- Levin, M. L., Schumacher, L. B. M. & Snellgrove, A. Effects of *Rickettsia amblyommatis* infection on the vector competence of *Amblyomma americanum* ticks for *Rickettsia rickettsii*. *Vector Borne Zoonotic Dis.* **18**, 579–587 (2018).
- Wu-Chuang, A. *et al.* Current debates and advances in tick microbiome research. *Curr. Res. Parasitol. Vector Borne Dis.* **1**, 100036 (2021).
- Kopáček, P., Hajdusek, O., Buresová, V. & Daffre, S. Tick innate immunity. *Adv. Exp. Med. Biol.* **708**, 137–162 (2010).
- Lalzar, I., Harrus, S., Mumcuoglu, K. Y. & Gottlieb, Y. Composition and seasonal variation of *Rhipicephalus turanicus* and *Rhipicephalus sanguineus* bacterial communities. *Appl. Environ. Microbiol.* **78**, 4110–4116 (2012).
- Tsementzi, D., Castro Gordillo, J., Mahagna, M., Gottlieb, Y. & Konstantinidis, K. T. Comparison of closely related, uncultivated *Coxiella* tick endosymbiont population genomes reveals clues about the mechanisms of symbiosis. *Environ. Microbiol.* **20**, 1751–1764 (2018).
- Maitre, A. *et al.* *Rickettsia helvetica* infection is associated with microbiome modulation in *Ixodes ricinus* collected from humans in Serbia. *Sci. Rep.* **12**, 11464 (2022).
- Maitre, A. *et al.* Rickettsial pathogens drive microbiota assembly in *Hyalomma marginatum* and *Rhipicephalus bursa* ticks. *Mol. Ecol.* **32**, 4660–4676 (2023).
- Guo, B. *et al.* Microbial co-occurrence network topological properties link with reactor parameters and reveal importance of low-abundance genera. *NPJ Biofilms Microbiomes* **8**, 3 (2022).
- Röttgers, L. & Faust, K. From hairballs to hypotheses—biological insights from microbial networks. *FEMS Microbiol. Rev.* **42**, 761–780 (2018).
- Estrada-Peña, A., Cabezas-Cruz, A. & Obregón, D. Behind taxonomic variability: The functional redundancy in the tick microbiome. *Microorganisms* **8**, 1829 (2020).
- Wu-Chuang, A., Obregon, D., Estrada-Peña, A. & Cabezas-Cruz, A. Thermostable keystone bacteria maintain the functional diversity of the *Ixodes scapularis* microbiome under heat stress. *Microb. Ecol.* **84**, 1224–1235 (2022).
- Narasimhan, S. *et al.* Gut microbiota of the tick vector *Ixodes scapularis* modulate colonization of the Lyme disease spirochete. *Cell Host Microbe* **15**, 58–71 (2014).
- Abraham, N. M. *et al.* Pathogen-mediated manipulation of arthropod microbiota to promote infection. *PNAS* <https://doi.org/10.1073/pnas.1613422114> (2017).
- Díaz-Sánchez, S., Estrada-Peña, A., Cabezas-Cruz, A. & de la Fuente, J. Evolutionary insights into the tick hologenome. *Trends Parasitol.* **35**, 725–737 (2019).
- Narasimhan, S. & Fikrig, E. Tick microbiome: The force within. *Trends Parasitol.* **31**, 315–323 (2015).
- Lejal, E. *et al.* Temporal patterns in *Ixodes ricinus* microbial communities: An insight into tick-borne microbe interactions. *Microbiome* <https://doi.org/10.1186/s40168-021-01051-8> (2021).
- Karim, S., Kumar, D. & Budachetri, K. Recent advances in understanding tick and rickettsiae interactions. *Parasite Immunol.* **43**, e12830 (2021).
- Namina, A. *et al.* Comparative microbiome analysis of three epidemiologically important tick species in Latvia. *Microorganisms* **11**, 1970 (2023).
- Van Treuren, W. *et al.* Variation in the microbiota of *Ixodes* ticks with regard to geography, species, and sex. *Appl. Environ. Microbiol.* **81**, 6200–6209 (2015).
- Ioffe-Uspensky, I., Mumcuoglu, K. Y., Uspensky, I. & Galun, R. *Rhipicephalus sanguineus* and *R. turanicus* (Acari:Ixodidae): closely related species with different biological characteristics. *J. Med. Entomol.* **34**(1), 74–81 (1997).
- Mumcuoglu, K. Y. *et al.* Pathogens in ticks collected in Israel: II. Bacteria and protozoa found in *Rhipicephalus sanguineus* sensu lato and *Rhipicephalus turanicus*. *Ticks Tick Borne Dis.* **13**, 101986 (2022).
- Sun, Y. *et al.* Severe fever with thrombocytopenia syndrome virus infection shapes gut microbiome of the tick vector *Haemaphysalis longicornis*. *Parasite Vectors* **17**, 107 (2024).
- de la Fuente, J. Overview: Ticks as vectors of pathogens that cause disease in humans and animals. *Front Biosci* **13**, 6938–6946 (2008).
- Lalzar, I., Friedmann, Y. & Gottlieb, Y. Tissue tropism and vertical transmission of *Coxiella* in *Rhipicephalus sanguineus* and *Rhipicephalus turanicus* ticks. *Environ. Microbiol.* **16**, 3657–3668 (2014).
- Socolovschi, C., Bitam, I., Raoult, D. & Parola, P. Transmission of *Rickettsia conorii conorii* in naturally infected *Rhipicephalus sanguineus*. *Clin. Microbiol. Infect.* **15**, 319–321 (2009).
- Matsumoto, K., Ogawa, M., Brouqui, P., Raoult, D. & Parola, P. Transmission of *Rickettsia massiliae* in the tick, *Rhipicephalus turanicus*. *Med. Vet. Entomol.* **19**, 263–270 (2005).

42. da Silva Costa, L. F., Nunes, P. H., Soares, J. F., Labruna, M. B. & Camargo-Mathias, M. I. Distribution of *Rickettsia rickettsii* in ovary cells of *Rhipicephalus sanguineus* (Latreille1806) (Acari: Ixodidae). *Parasites Vectors* <https://doi.org/10.1186/1756-3305-4-222> (2011).
43. Duron, O. *et al.* The recent evolution of a maternally-inherited endosymbiont of ticks led to the emergence of the Q fever pathogen, *Coxiella burnetii*. *PLoS Pathog.* **11**, e1004892 (2015).
44. Oña, L. & Kost, C. Cooperation increases robustness to ecological disturbance in microbial cross-feeding networks. *Ecol. Lett.* **25**, 1410–1420 (2022).
45. Weese, J. S. The canine and feline skin microbiome in health and disease. *Vet. Dermatol.* **24**, 137–e31 (2013).
46. Estrada-Peña, A., Cabezas-Cruz, A. & Obregón, D. Resistance of tick gut microbiome to anti-tick vaccines, pathogen infection and antimicrobial peptides. *Pathogens* **9**, 309 (2020).
47. Mateos-Hernández, L. *et al.* Anti-microbiota vaccines modulate the tick microbiome in a taxon-specific manner. *Front. Immunol.* <https://doi.org/10.3389/fimmu.2021.704621> (2021).
48. He, X., McLean, J. S., Guo, L., Lux, R. & Shi, W. The social structure of microbial community involved in colonization resistance. *ISME J.* **8**, 564–574 (2014).
49. Swei, A. & Kwan, J. Y. Tick microbiome and pathogen acquisition altered by host blood meal. *ISME J.* **11**, 813–816 (2016).
50. Driscoll, T. P. *et al.* Wholly *Rickettsia!* Reconstructed metabolic profile of the quintessential bacterial parasite of eukaryotic cells. *mBio* <https://doi.org/10.1128/mBio.00859-17> (2017).
51. Alasmari, S. & Wall, R. Metabolic rate and resource depletion in the tick *Ixodes ricinus* in response to temperature. *Exp. Appl. Acarol.* **83**, 81–93 (2021).
52. An, L. *et al.* The microbiota changes of the brown dog tick, *Rhipicephalus sanguineus* under starvation stress. *Front. Physiol.* **13**, 932130 (2022).
53. Della Noce, B. *et al.* Carbohydrate metabolic compensation coupled to high tolerance to oxidative stress in ticks. *Sci. Rep.* **9**, 4753 (2019).
54. Villar, M. *et al.* Integrated metabolomics, transcriptomics and proteomics identifies metabolic pathways affected by *Anaplasma phagocytophilum* infection in tick cells. *Mol. Cell. Proteomics* **14**, 3154–3172 (2015).
55. Cabezas-Cruz, A., Alberdi, P., Valdés, J. J., Villar, M. & de la Fuente, J. *Anaplasma phagocytophilum* infection subverts carbohydrate metabolic pathways in the tick vector, *Ixodes scapularis*. *Front. Cell. Infect. Microbiol.* **7**, 23 (2017).
56. Meyer, F. *et al.* The metagenomics RAST server—A public resource for the automatic phylogenetic and functional analysis of metagenomes. *BMC Bioinform.* **9**, 386 (2008).
57. Cox, M. P., Peterson, D. A. & Biggs, P. J. S. SRA: At-a-glance quality assessment of Illumina second-generation sequencing data. *BMC Bioinform.* **11**, 485 (2010).
58. Gomez-Alvarez, V., Teal, T. K. & Schmidt, T. M. Systematic artifacts in metagenomes from complex microbial communities. *ISME J.* **3**, 1314–1317 (2009).
59. Wilke, A. *et al.* The M5nr: A novel non-redundant database containing protein sequences and annotations from multiple sources and associated tools. *BMC Bioinform.* **13**, 141 (2012).
60. O’Leary, N. A. *et al.* Reference sequence (RefSeq) database at NCBI: Current status, taxonomic expansion, and functional annotation. *Nucleic Acids Res.* **44**, D733–745 (2016).
61. Randle-Boggis, R. J., Helgason, T., Sapp, M. & Ashton, P. D. Evaluating techniques for metagenome annotation using simulated sequence data. *FEMS Microbiol. Ecol.* **92**, fiw095 (2016).
62. Bray, J. R. & Curtis, J. T. An ordination of the upland forest communities of southern wisconsin. *Ecol. Monogr.* **27**, 325–249 (1957).
63. Oksanen, J. *et al.* vegan: community ecology package. R package version 2.6–5 (2024).
64. RStudio Team. *RStudio: Integrated Development Environment for R* (RStudio, PBC, 2020).
65. Dhariwal, A. *et al.* MicrobiomeAnalyst: A web-based tool for comprehensive statistical, visual and meta-analysis of microbiome data. *Nucleic Acids Res.* **45**, W180–W188 (2017).
66. Chen, H. VennDiagram: generate high-resolution venn and euler plots. R package version 1.7.3 (2022).
67. Fernandes, A. D., Macklaim, J. M., Linn, T. G., Reid, G. & Gloor, G. B. ANOVA-like differential expression (ALDEx) analysis for mixed population RNA-Seq. *PLoS One* **8**, e67019 (2013).
68. Benjamini, Y. & Hochberg, Y. Controlling the false discovery rate: A practical and powerful approach to multiple testing. *J. R. Stat. Soc. B Stat. Methodol.* **57**, 289–300 (1995).
69. Warnes, G. R. *et al.* gplots: Various R programming tools for plotting data. R package version 3.1.3.1 (2024).
70. Friedman, J. & Alm, E. J. Inferring correlation networks from genomic survey data. *PLoS Comput. Biol.* **8**, e1002687 (2012).
71. Faust, K. & Raes, J. Microbial interactions: From networks to models. *Nat. Rev. Microbiol.* **10**(8), 538–550 (2012).
72. Bastian, M., Heymann, S. & Jacomy, M. Gephi: An open source software for exploring and manipulating networks. *Proc. Int. AAAI Conf. Web. Soc. Media* **3**, 361–362 (2009).
73. Röttjers, L., Vandeputte, D., Raes, J. & Faust, K. Null-model-based network comparison reveals core associations. *ISME Commun.* **1**, 36 (2021).
74. Real, R. & Vargas, J. The probabilistic basis of Jaccard’s index of similarity. *Syst. Biol.* **45**, 380–385 (1996).
75. Peschel, S., Müller, C. L., von Mutius, E., Boulesteix, A.-L. & Depner, M. NetCoMi: Network construction and comparison for microbiome data in R. *Brief. Bioinform.* **22**, bbaa290 (2021).
76. Lhomme, S. Analyse spatiale de la structure des réseaux techniques dans un contexte de risques. *Cybergeol* <https://doi.org/10.4000/cybergeol.26763> (2015).
77. Freitas, S., Yang, D., Kumar, S., Tong, H. & Chau, D. H. *Evaluating Graph Vulnerability and Robustness using TIGER* (ACM Digital Library, 2020).
78. Csárdi, G. *et al.* igraph: Network analysis and visualization. R package version 2.0.2 (2024).
79. Csárdi, G. & Nepusz, T. The igraph software package for complex network research. *Comput. Sci. Eng.* **1695**(5), 1–9 (2006).
80. Love, M. I., Huber, W. & Anders, S. Moderated estimation of fold change and dispersion for RNA-seq data with DESeq2. *Genome Biol.* **15**, 550 (2014).

Acknowledgements

UMR BIPAR is supported by the French Government’s Investissement d’Avenir program, Laboratoire d’Excellence “Integrative Biology of Emerging Infectious Diseases” (grant no. ANR-10-LABX-62-IBEID). Apolline Maitre is supported by the ‘Collectivité de Corse’, grant: ‘Formations superieures’ (SGCE – RAPPORT N° 0300).

Author contributions

Conceptualization: AC-C and DO. Supervision: AC-C. Data Curation: LM-H and DO. Formal Analysis: AM, MK, IC-G, LA-D, EP-S and DO. Methodology and Software: AM, LA-D and DO. Visualization: AM and DO. Writing – Original Draft Preparation: AM, MK and AC-C. Writing – Review & Editing: AM, MK, IC-G, LA-D, LM-H, JM, CA, MBS, EP-S, DO and AC-C. All authors wrote and discussed the results, commented on the manuscript and approved the submitted version.

Competing interests

The authors declare no competing interests.

Additional information

Supplementary Information The online version contains supplementary material available at <https://doi.org/10.1038/s41598-024-71539-4>.

Correspondence and requests for materials should be addressed to D.O. or A.C.-C.

Reprints and permissions information is available at www.nature.com/reprints.

Publisher's note Springer Nature remains neutral with regard to jurisdictional claims in published maps and institutional affiliations.

Open Access This article is licensed under a Creative Commons Attribution-NonCommercial-NoDerivatives 4.0 International License, which permits any non-commercial use, sharing, distribution and reproduction in any medium or format, as long as you give appropriate credit to the original author(s) and the source, provide a link to the Creative Commons licence, and indicate if you modified the licensed material. You do not have permission under this licence to share adapted material derived from this article or parts of it. The images or other third party material in this article are included in the article's Creative Commons licence, unless indicated otherwise in a credit line to the material. If material is not included in the article's Creative Commons licence and your intended use is not permitted by statutory regulation or exceeds the permitted use, you will need to obtain permission directly from the copyright holder. To view a copy of this licence, visit <http://creativecommons.org/licenses/by-nc-nd/4.0/>.

© The Author(s) 2024